Paper No. 1596. (quote when citing this article)
Eleventh World Conference on Earthquake Engineering
ISBN: 0 08 042822 3

NONLINEAR CHARACTERISTICS OF GROUND CONSTRAINT ON BURIED PIPES CAUSED BY LATERAL DISPLACEMENT DURING EARTHQUAKES

H. ANDO and M. KOBAYASHI

Fundamental Technology Research Laboratory, Tokyo Gas Co., Ltd.,
16-25, Shibaura, 1-chome, Minato-ku, Tokyo, 105, JAPAN

ABSTRACT

To date, very few extensive examinations have been conducted on the ground constraints on buried pipes that take place when the ground experiences lateral displacement, such as landslides and lateral flow which is caused by liquefaction during earthquakes. Therefore, a full-scale experiment was carried out in an experimental pit to evaluate the characteristics of ground constraint. The results of the experiment suggest that the ground constraint peaks when the relative displacement between ground and pipe was very small, and that beyond that level, the ground constraint level begins to decline. The experiment results also verified that as long as the sand's mechanical characteristics remain unchanged, the maximum ground constraint level and the critical displacement can be defined by the ratio between the pipe's burial depth and its diameter. The ground constraint model could be approximated by a hyperbola, which suggested that these findings could be easily applied to the design. A verification analysis using FEM indicated that the characteristics obtained by the experiment can be reproduced at a level of precision that will enable successful commercial application. This created the possibility that constraint characteristics will be reproduced more systematically.

KEYWORDS

Buried pipe; Earthquake; Ground constraint; Liquefaction; Lateral displacement; Full scale experiment

INTRODUCTION

For relatively low levels of earthquake-induced ground displacement, the ground constraint applied to linear underground structures such as underground pipes is generally evaluated using a spring model, which simulates the ground behavior in the proximity of the underground objects. This enables analysis of targeted structures often used under the response displacement method as the beams on an elastic foundation, as well as an evaluation of the deformation. In a previously introduced design(Japan gas association, 1982) that takes into consideration the slippage between the ground and the pipe, ground constraint was assessed in the pipe's axial direction. For ground constraint in the pipe's longitudinal direction, the experimental and analytical examinations conducted thus far have assessed longitudinal displacement in the form of ground subsidence. In this respect, an assessment method that employs the results of a plate bearing experiment has already been established(Shimamura et al., 1987, hyodo et al., 1991). However, there have been virtually no extensive examinations on lateral ground displacement such as landslides or lateral flows caused by liquefaction during earthquakes, with the exception of experiments such as that conducted by Trautmann et al.(1985).

Therefore a full-scale experiment was performed in an experimental pit. By comparing the results obtained with Trautmann's results, it could be assessed that the ground constraint applied to pipes embedded horizontally and longitudinally relative to the axis. Ground analysis using FEM was also conducted, and the adaptability of the numerical analysis method was examined.

EXPERIMENT METHOD

As Figure 1 shows, the experiment was performed under the assumption that the ground experienced lateral displacement. It was also assumed that even when the ground displacement resulted from liquefaction, the pipe remained embedded in a non-liquefied layer. Such factors as the decrease in ground rigidity resulting from the rise in excess pore water pressure was not taken into consideration. Figure 2 shows outlines of the experiment devices and instrumentations. Photograph 1 shows a scene of the experiment.

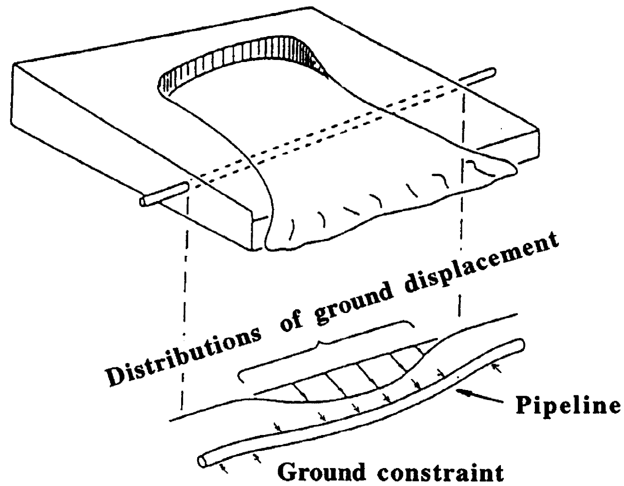

Figure 1 Example of lateral ground displacement.

The pit used for the experiment is made of concrete, and is 5m long, 2m wide, and 2.1m deep, for a volumetric capacity of 21m^3. The pipes embedded were made of uncoated steel (STPG370), and were 1.9m in length. Pipe diameters of 600A, 300A and 150A were used with outer diameters of 609.6, 318.5 and 165.2mm, respectively. The pipes were embedded to a depth of 1.5m, as measured from the ground surface to the pipe center, which is almost equivalent to the depth of regular gas pipelines. The pipes were then covered with fine sand, which was compacted by a roller at 30cm depth intervals. Backfilling was performed in this manner to ensure that the degree of compaction reached a minimum 95%. The characteristics of the fine sand were as follows: water content ratio w, approximately 11%; wet unit weight γ t, 1.73 gf/cm^3; average grain size D_{50}, 0.31; and uniformity coefficient Uc, 2.8. The results of the triaxial compression test indicated an internal friction angle of 45.8 and cohesion C of 0.05.

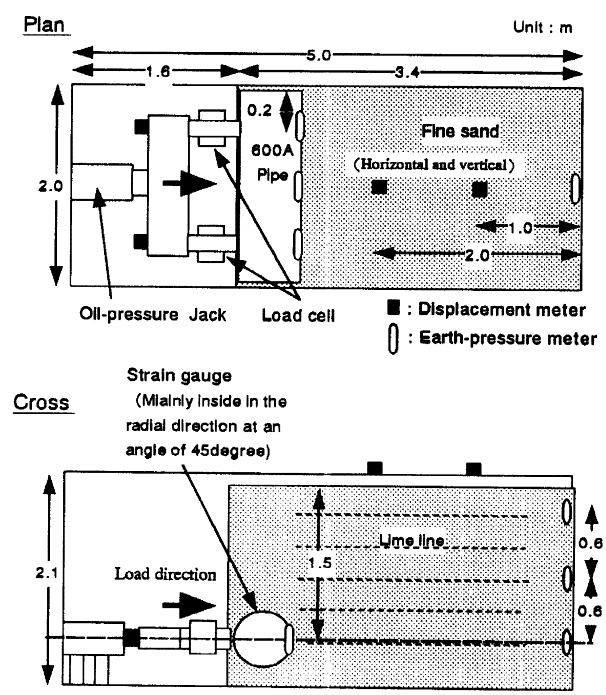

Figure 2 Experimental devices and instrumentations.

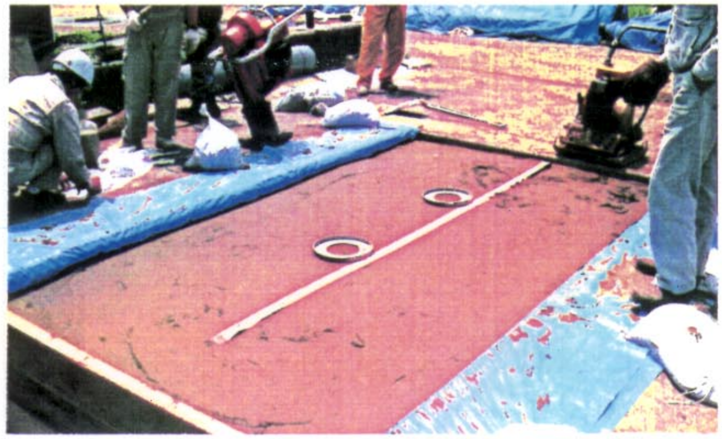

Photograph 1 Scene of experiment.

The experiment was conducted by applying to the pipe a displacement speed of approximately 0.3cm/sec, using an oil-pressure jack, until relative displacement reached a maximum of 25cm. The relationship between the ground constraint and the displacement was measured using the load cell and the displacement meter, both of which were installed in the section between the jack and the pipe. In addition, the soil pressures on the center of the pipe surface and on the concrete wall, and the displacement of the pipe itself, all of which are shown in Figure 1, were measured using a soil pressure gauge, as well as the strain gauge attached to the inside of the pipe. At the same time, to observe the level of deformation during, for example, a landslide, lime was spread each time the soil was compacted. To minimize the friction between the soil and the wall at the pipe end, two layers of plastic sheets were laid, applying a coating of grease to the sheet surfaces where they were in contact with each other.

Three experiment models were set up as follows: pipes of diameters 600A, 300A and 150A were embedded to a depth of 1.5m. Two experiments were performed for each model. To assess the firmness with which the pipes were embedded in the soil, it was conducted that one experiment on the 150A diameter pipe, after had first been left for about a week after being embedded. The results of this experiment revealed no significant differences in soil firmness, due to the low cohesion of the sand used for the experiment. Therefore, the other models were left overnight prior to assessment.

EXPERIMENTAL RESULTS

Figure 3 shows the experiment results. Here, the relative displacement δ between the soil and pipe refers to δ' (δ/H), the ratio of embedment depth, H. The ground constraint was expressed by the ratio F' (F/γ tHDL), which relates the constraint of unit area σ (F/DL), obtained by dividing load F by D x L, and the vertical soil pressure γ tH. Therefore non-dimensional values were adopted.

The results revealed that when displacement was augmented, constraint increased significantly, producing an evident peak in all cases. After the peak, constraint declined, even when displacement was augmented. The results of the experiments involving the pipe of 600A diameter suggest that after the constraint ratio F' peaked at approximately 9.4 (F=approx. 30 x 10^3kgf), obtained at a displacement ratio δ' of approximately 0.02 (δ =approx. 3cm), constraint gradually declined. All models yielded similar results in the first and second round of experiments, pointing to an high level of accuracy in experimental reproduction.
It was discovered that the maximum ground constraint ratio F'max, tended to increase as the ratio, H/D, between the embedment depth and the diameter, also increased. It was also confirmed that the critical displacement ratio δ'cr remained constant at approximately 0.02, regardless of the value of H/D. In the experiment conducted by Trautmann et al., maximum pipe diameter was 300A, with varying sand densities

and internal friction angles. The results from that experiment resemble the results obtained in this experiment, where an internal friction angle of 45 was used, suggesting that the pit soil is of high quality. This experiment would seem to have demonstrated that even when pipe diameter increases, the constraining force applied to the pipe in the longitudinal direction under lateral soil displacement can be assessed using the ratio H/D, which relates embedment depth and pipe diameter.

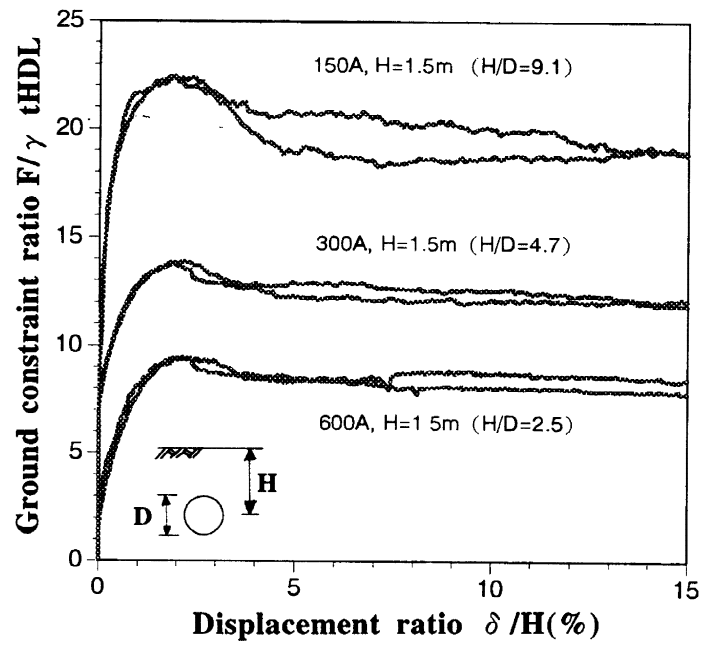

Figure 3 Ground constraint and displacement by the experiment.

It was also found out that the ground constraint possesses strong nonlinear characteristics. As Photograph 2 shows, in all cases, numerous cracks were seen on the ground surface along the axial direction of the pipe as the load applied to the pipe increased during the experiment. Furthermore, in post-experiment observations of the lime lines in the cross-section of the pit, which followed the excavation of half the length of the pit, there were still visible signs of a ground sliding that took place in a section located at angle of approximately 45 from the pipe leading to the ground surface, as shown in Photograph 3. This accordingly produced differences in elevation on the ground surface. However, it were be unable to witness any landslides in the region near the pipe. The ground surface directly over the pipe experienced no differences in elevation from the underground sliding, though it were found that signs of heaving and disorientation in the direction of the load. It appears that the soil critical in this area, particularly in the area of the landslide, caused strong non-linearity in the constraint characteristics.

Photograph 2 Ground surface cracks occurred.

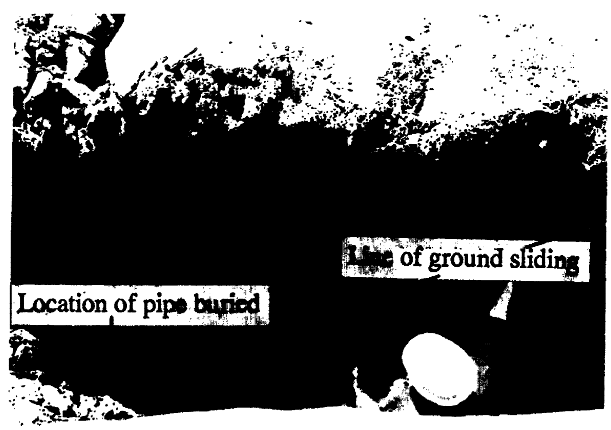

Photograph 3 Ground sliding failure occurred.

COMPARISON WITH NUMERICAL ANALYSIS

To verify the ground constraint behavior witnessed in the experiment, a model was built ,which adopted the finite element method(FEM), using the soil and the pipe. Then numerical analysis was performed using the general FEM analysis code "ABAQUS". Based on the results of the triaxial compression test, the following soil properties were estimated and assigned: Young's modulus Eg, 437kgf/cm^2; and Poisson's ratio μ , 0.38. Other values were used unmodified. Based on the Mohr-Coulomb failure criterion, the non-linear characteristics of the soil elements were approximated by the perfectly elastic-plastic model. As the strain experienced by the pipe in the direction of its circumference registers a maximum 0.2% (for a pipe with 300A diameter), which falls within the range of allowable elasticity and suggests that deformation will be small, a pipe was used with rigid properties. Joint elements were used on the boundary between the soil and the pipe, in order to ensure that compaction stress alone worked in the perpendicular direction to the pipe circumference and thus to prevent any separation between the pipe and the soil. Figure 4 shows a comparison between the experimental and analytical results for the unit-area relationship between the ground constraint σ and displacement δ for all models.

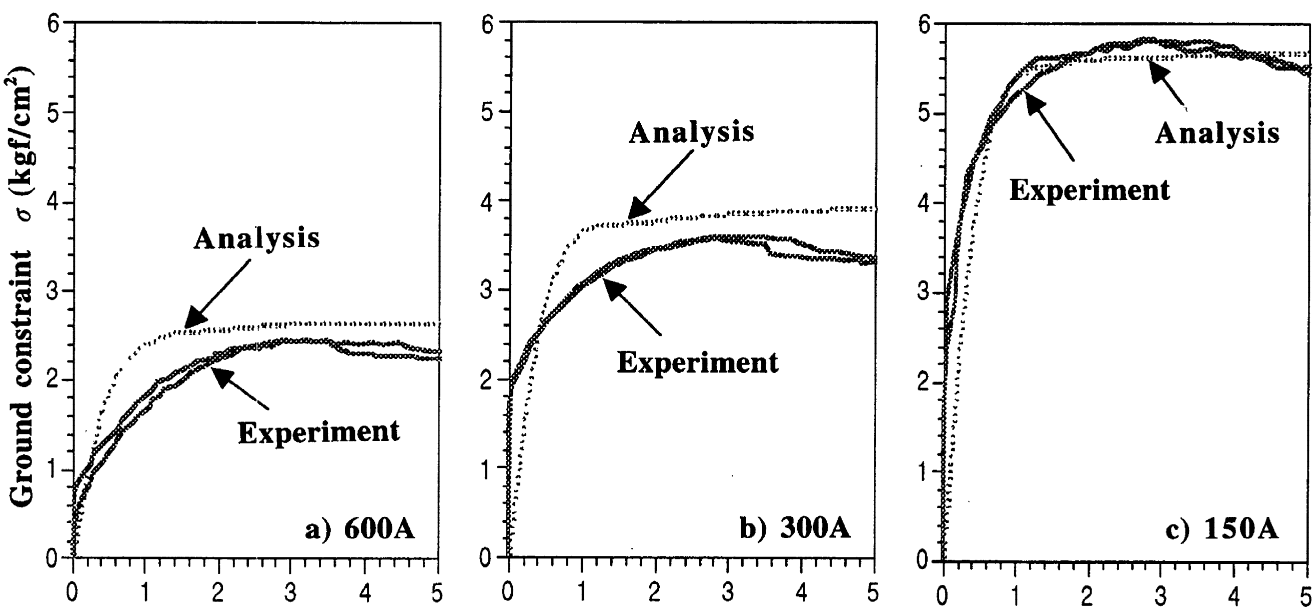

Figure 4 Comparison of experimental and analytical results.

These results show that the two sets of results closely resemble each other for all models. Figure 5 shows the soil displacement recorded when the pipe displacement δ is 0.4cm and 2.0cm, the point at which the constraint level peaks, as well as the main stress and distribution of plastic strain.
These results indicate that when pipe displacement increased, soil deformation in proximity to the pipe becomes more manifest, and that this change is accompanied by higher values for soil stress in the direction of compaction in this same area. This trend was extremely prevalent in the soil located at 45degree from the loading direction. The plastic strain distribution was seen leading from the pipe, and diagonally and upward from the loading direction when the displacement δ was 0.4cm. This distribution almost matched the slip line confirmed by the experiment. Furthermore, when the displacement increased, the area experiencing the plastic strain expanded. The results of analysis verified that virtually all the soil experienced a certain level of plasticity when the displacement δ reached 2.0 cm at the same time that the average soil constraint on the pipe peaked.

As these results suggest, the non-linear characteristics of the soil obtained by the experiment were evident in the analysis as well. This finding indicated that the maximum ground constraint, critical displacement, and other factors can be reproduced at an accuracy that enables commercial application.

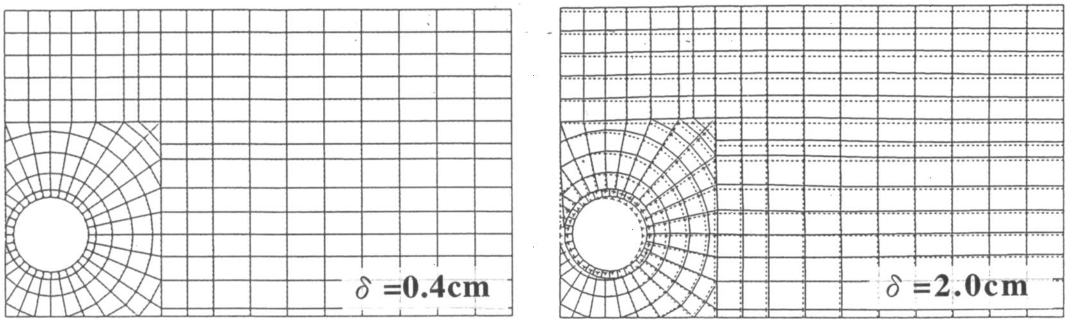

a) Soil displacement

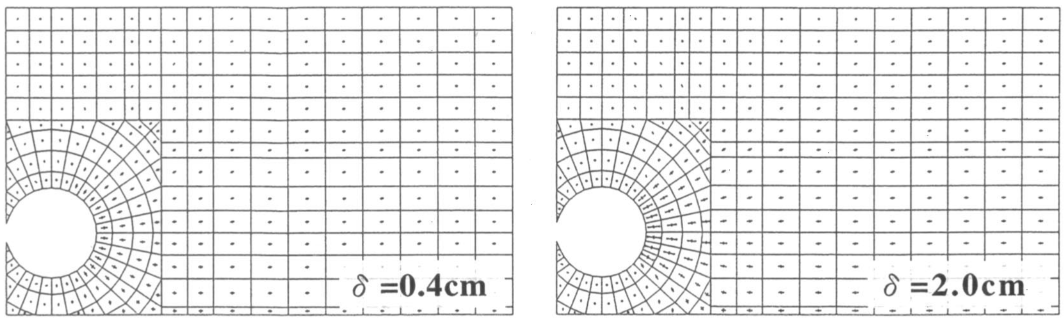

b) Soil main stress

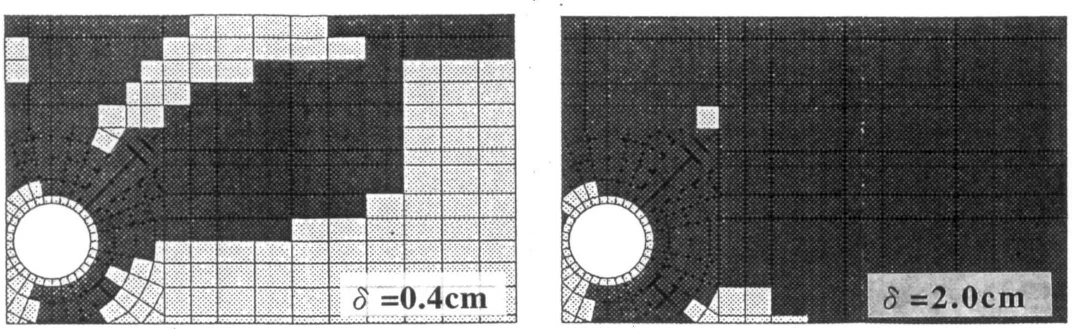

c) Plastic strain(dark zone)

Figure 5 Distributions of soil displacement, main stress and plastic strain recorded when the pipe displacement δ is 0.4cm and 2.0cm by analysis.

METHOD OF ASSESSING GROUND CONSTRAINT

Maximum ground constraint and critical displacement

Based on the experiment results described above, Figure 6 shows the relationship between the maximum ground constraint ratio F' max (Fmax/γ tHDL), the ratio δ cr/H which relates critical displacement and embedment depth and the ratio H/D which relates embedment depth and the pipe diameter. Here, it was also provided that the results from the experiment conducted by Trautmann et al., at an internal friction angle of 45degree, which is almost equivalent to the condition of the soil used for the experiment.

The results show that when the H/D, the ratio between the embedment depth and the pipe diameter, increased, the maximum constraint ratio F' max also increased. In contrast, the critical displacement ratio δ cr/H remained virtually unchanged regardless of the value of H/D. These tendencies matched those found by Trautmann et al. Although Trautmann et al. set the relationship between the critical displacement and embedment depth under the above soil conditions at δ cr=0.03H, the authors adopted a slightly lower value of approximately 0.02H.

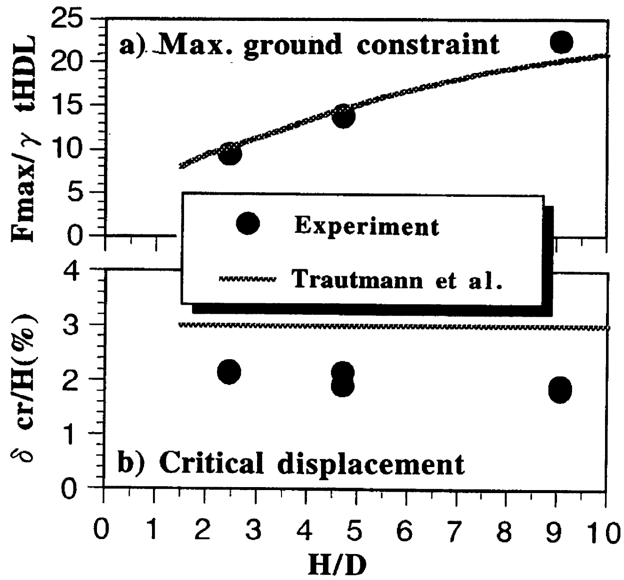

Figure 6 Maximum ground constraint ratio F'max , the ratio δ cr/H and the ratio H/D.

Ground Constraint Model

Here, it was examined that the ground constraint model used for the design. Based on the experiment results, the ground constraint was defined as F"=F'/F'max, and the relative displacement between the pipe and the soil defined as δ ''= δ '/ δ 'cr. Figure 7 shows the results produced by the model. It was also combined that the results of experiments involving three types of sand: highly dense sand like that used for this experiment, rather loose sand, and sand with a level of concentration that lies between the two. A regression equation F''= δ ''/(0.17+0.83 δ '') was developed, using the hyperbola shown by Trautmann et al.

The results indicate that the relationship between the ground constraint and displacement obtained from this experiment closely resembles Trautmann's hyperbola model. It was believed that this enables to be assess ed the constraint working along the longitudinal axis of an embedded pipe in relation to the soil's lateral displacement. Furthermore, during the design for earthquake resistance, the same constraint can be ideally approximated by using a hyperbola with a bilinear model. Thomas et al.(1978), therefore, proposed a model which peaks at F'/F'max=70%. The model achieves the relationship shown by the broken lines shown in the figure. Based on this relationship, it was calculated that the design critical displacement δ crd (cm), the constraint coefficient kd(kgf/cm^3), and the maximum ground constraint σ crd (kgf/cm^2), for a pipe of 600A diameter embedded to a depth of 1.5m. F'max, the maximum ground constraint, and the other values were adopted from the results of experiments by Trautmann el al., as shown in Figure 6. The results produced were δ crd=1.8cm, kd=1.4kgf/cm^3, and σ crd=2.6kgf/cm^2.

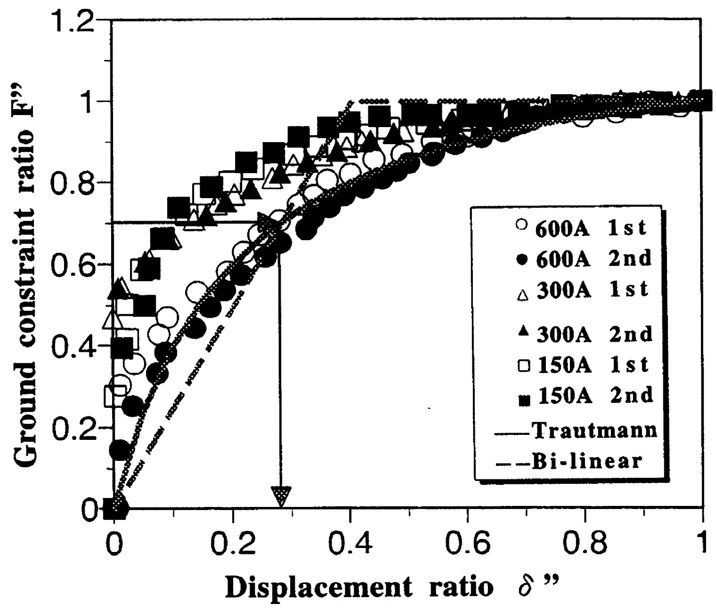

Figure 7 Ground constraint model using a hyperbola.

CONCLUSIONS

Assuming a major soil displacement entered an embedded pipe in horizontal and longitudinal directions to the pipe axis, the constraint which the soil places on the pipe was examined by conducting a full-scale experiment using a pipe of a maximum 600A diameter, as well as a numerical analysis. Then the method of assessing the ground constraint model was examined. The results were as follows:

The ground constraint increases significantly in accordance with increases in displacement. The ground constraint peaks in a narrow displacement level, and then gradually declines. This pattern is believed to result from a rise in the soil triggered by a slip line running from the area near the pipe to the ground surface, which was detected after the experiment, as well as the many cracks in the soil that appeared on the ground surface.

While the experiment verified that an increase in the ratio between the embedment depth and the pipe diameter led to an increase in the maximum ground constraint ratio, and that the ratio of critical displacement remained almost unchanged regardless of the H/D value, the ratio between the embedment depth and the pipe diameter. This result closely resembles that obtained by Trautmann.

Our findings suggested that ground constraint behavior can be assessed, by using FEM numerical analysis, at a level of accuracy that enables commercial application. It is also possible to identify the ground constraint while taking into consideration the different soil properties and embedment conditions, even in soil conditions other than used in this experiment.

The ground constraint can be approximated by a hyperbola model. This also allows conversion into a bilinear model used for design.

REFERENCES

Tomas, H.O. (1978). Discussion of "Soil Restraint Horizontal Motion of Pipe, *Journal of the Geotechnical Engineering Division*, ASCE, Vol.10, No.GT9, 1214-1216

Japan Gas Association. (1982). Recommended Practice for Earthquake Resistant Design of Gas Pipeline (in Japanese)

Trautmann, C. H., Tomas, D.O. (1985). Lateral Force-Displacement Response of Buried Pipe, *Journal of Geotechnical engineering,* ASCE, Vol.111, No.9, 1077-1092

Shimamura, K., Nishio, N., Takagi, N., Hyodo, M. (1987). Earth Pressure on Buried Pipes under projection Condition, Proc. of JSCE, No.388,179-188 (in Japanese)

Hyodo, M., Shimamura, K., Takagi, N., (1991). Field Test and Analysis for Evaluating a Coefficient of Subgrade Reaction for buried Pipes, *Tsuchi-to-Kiso*, No.399, 3-8 (in Japanese)